High-Vacuum Vapor Deposition and in Situ Monitoring of N-Carboxy Anhydride Benzyl Glutamate Polymerization

ARTICLE *in* LANGMUIR · AUGUST 2009

Impact Factor: 4.46 · DOI: 10.1021/la9012125 · Source: PubMed

7 AUTHORS, INCLUDING:

Hatice Duran
TOBB University of Economics and Technology
40 PUBLICATIONS **512** CITATIONS
SEE PROFILE

Hiroaki Usui
Tokyo University of Agriculture and Technol…
68 PUBLICATIONS **427** CITATIONS
SEE PROFILE

Rigoberto C. Advincula
Case Western Reserve University
352 PUBLICATIONS **7,266** CITATIONS
SEE PROFILE

Langmuir
Article
pubs.acs.org/Langmuir

High-Vacuum Vapor Deposition and in Situ Monitoring of *N*-Carboxy Anhydride Benzyl Glutamate Polymerization

Hatice Duran,[†] Kenta Ogura,[‡] Kenji Nakao,[‡] Sulivan D. B. Vianna,[†] Hiroaki Usui,*[,‡] Rigoberto C. Advincula,*[,§] and Wolfgang Knoll*[,†,∥]

[†]*Max Planck Institute for Polymer Research, Ackermannweg 10, Mainz, D-55128 Germany,* [‡]*Department of Organic and Polymer Materials Chemistry, Tokyo University of Agriculture and Technology, Naka-Cho, Koganei, Tokyo 184-8588, Japan, and* [§]*Department of Chemistry and Department of Chemical Engineering, University of Houston, Houston, Texas 77204-5003.* [∥]*Current address: Austrian Institute of Technology, Danau-City-Strasse 1, 1220 Vienna, Austria.*

Received April 6, 2009. Revised Manuscript Received June 27, 2009

A high-vacuum physical vapor deposition (PVD) method was used to grow polypeptide chains from gold surfaces coupled with in situ monitoring using surface plasmon resonance spectroscopy (SPR). Polymerization of *N*-carboxy anhydride of benzyl-L-glutamate (BLG-NCA) was demonstrated, forming grafted polybenzyl-L-glutamate (PBLG) films. 2-Aminoethanethiol (AET) was used as the initiating site either deposited as a self-assembled monolayer (SAM), as a PVD film, or codeposited on the gold substrates. PBLG films up to 30 nm thick in which the formation of different secondary structures was monitored by in situ SPR and ex situ Fourier transform infrared spectroscopy (FT-IR) methods based on the parameters for deposition were prepared. Furthermore, surface topology and film morphology properties were determined on the basis of AFM measurements and were found to depend largely on the deposition process of the AET. Besides investigation of the AET surface density effects, the orientation of the PBLG chains was also characterized using ex situ FT-IR.

Introduction

Polypeptides are known to form hierarchically ordered structures with α-helices (stabilized by intramolecular H-bonds) and β-sheets (stabilized by intermolecular H-bonds) being their fundamental secondary motifs. The α-helical structure, in particular, is thought to give rise to rigid-rod structures. In this respect, poly(γ-benzyl-L-glutamate) (PBLG) has been employed as a model rigid-rod polymer with interesting macromolecular properties in solution, in the melt, and on surfaces.[1] A nonlinear optical response, based on second harmonic generation (SHG), can be expected in a monomolecular polyglutamate film that has a unidirectional orientation of the polymer backbones.[2] An approach to such a unidirectional orientation of the polypeptide helices is the covalent attachment of one of the polymer chain end groups to the substrate with high grafting density.

Surface-attached synthesis of the chemisorbed polypeptide chains by polymerization from amino acid *N*-carboxy anhydrides (NCA) has been demonstrated for some time now.[3,4] Polypeptide self-organization occurring at surfaces and interfaces can, in principle, be different from that observed in the bulk. Indeed, the formation of reversible hydrogen bonding arrays and the corresponding secondary structures can be influenced by adsorption and sufficient high surface coverage by the grafted chains as well. Such surface effects play an important role in protein stability and function as, for example, in biomimetic steps in biomineralization processes.[5] In addition, the morphology of the polypeptide film can be very different in solution and on the surface because of the dominant role of the substrate in surface self-assembly.[6] Moreover, tethered rodlike synthetic polypeptides with a controlled orientation and molecular conformation have potential applications in liquid crystal displays,[7] biosensors,[8,9] optical switches,[10] and piezoelectric[11] and nonlinear optics.[12]

For polypeptide grafting reactions that started from the surface, it is necessary that the initiator remain attached to the polymer. This was achieved by starting the polymerization with a self-assembled monolayer (SAM) of primary amines (i.e., thiole or silane) from dilute solutions (DMF, THF, or dioxane). The carboxyl anhydride groups of the monomer react first with the surface-tethered amine groups through ring opening polymerization to form amide bond linkages with subsequent release of carbon dioxide, leaving the free amines on the other end of the growing chains. Because of several side reactions, such as nucleophilic attack on C-2 leading to an inactive chain end[4] or self-cyclization of the chains or chemical deactivation of the end groups,[13] the maximum value of the

*To whom correspondence should be addressed. E-mail: radvincula@uh.edu, h_usui@cc.tuat.ac.jp, and wolfgang.knoll@arcs.ac.at.

(1) Block, H. *Poly(γ-benzyl-L-glutamate) and Other Glutamic Acid containing Polymers*, 1st ed.; Gordon and Breach Science Publishers Inc.: New York, 1983.
(2) (a) Mitchell, S. A.; McAloney, R.; Moffatt, D.; Mora-Diez, N.; Zgierski, M. *J. Chem. Phys.* **2005**, *122*, 114707. (b) Yen, C.; Taguchi, Y.; Tokita, M.; Watanabe, J. Macromolecules **2008**, *41*, 2755–2758.
(3) (a) Chang, Y.-C.; Frank, C. W. *Langmuir* **1996**, *12*, 5824–5829. (b) Kurita, K.; Kanari, M.; Koyama, Y. Polym. Bull. **1985**, *14*, 511.
(4) Oosterlin, M. L. C. M.; Willems, E.; Schouten, A. J. *Polymer* **1995**, *36*, 4463–4470.
(5) Mann, S. *Nature* **1988**, *332*, 119.
(6) Kitaev, V.; Kumacheva, E. *Langmuir* **1998**, *14*, 5568–5572.
(7) Naijo, Y.; Ikeda, K.; Tsunoda, M.; Tanaka, T.; Kobayashi, N. *Mol. Cryst. Liq. Cryst.* **2003**, *406*, 381–387.
(8) (a) Duran, H.; Lau, K. H. A.; Lübbert, A.; Jonas, U.; Steinhart, M.; Knoll, W. Biopolymers for Biosensors: Polypeptide nanotubes for Optical Biosensing. In *Polymers for Biomedical Applications*; Mahapatro, A., Kulshresha, A. S., Eds.; American Chemical Society Book Series 977; Oxford University Press: New York, 2008; Chapter 22.(b) Duran, H.; Lau, K. H. A.; Jonas, U.; Knoll, W. *Polym. Mater.: Sci. Eng.* **2006**, *95*, 345–347.
(9) Deming, T. *Adv. Mater.* **1997**, *9*, 299–311.
(10) Ciardelli, F.; Pieroni, O. Photoswitchable polypeptides. In *Molecular Switches*; Wiley-VCH Verlag GmbH: Berlin, 2001; pp 399−441.
(11) Jaworek, T.; Neher, G.; Wegner, G.; Wieringa, R. H.; Schouten, A. J. *Science* **1998**, *279*, 57.
(12) Whitesell, J. K.; Chang, H. K. *Mol. Cryst. Liq. Cryst.* **1994**, *240*, 251.
(13) Wang, W.; Chang, Y.-C. *Langmuir* **2002**, *18*, 9859–9866.

thickness of the polymer chains is usually limited to tens of nanometers (degree of polymerization DPn ≤ 100). Alternatively, Frank and Chang[14] have demonstrated the preparation of polypeptide films via a vapor phase deposition from amine-functionalized (initiator) substrates giving higher-molecular weight derivatives. Their approach involves investigating the use of the dry deposition process under low vacuum (26.6−5.33 Pa) and high temperatures (95−125 °C). Following their work, in a series of experiments, Frank et al.[15] and Chang et al.[13,16−18] conducted high-vacuum vapor deposition for a wide range of α-amino acid monomers on Si_2O substrates. Using an approach similar to theirs, here, we present the use of high-vacuum physical vapor deposition (PVD) of *N*-carboxy anhydride of the benzyl-L-glutamate (BLG-NCA) monomer on gold substrates to introduce polymeric materials "grafted from" surfaces.[19] The primary goal of this work is to use the PVD to prepare highly oriented polypeptides on gold surfaces in a totally dry process and monitor the growth process in situ. In this work, film deposition of the initiator, which is difficult to condense on the substrate surface by the conventional PVD, was also made possible by the aid of a hot filament-assisted PVD technique.[20] Surface grafting of PBLG via the PVD technique was monitored in situ by surface plasmon spectroscopy (SPR) by varying initiator and BLG-NCA monomer deposition conditions: (i) SAM of the initiator layer and PVD of the BLG-NCA monomer, (ii) PVD of the initiator molecule followed by PVD of the BLG-NCA monomer, and (iii) co-evaporation of both the initiator and BLG-NCA monomer by PVD. The concept of co-evaporation was introduced for the first time in this research study. SPR is a powerful yet experimentally simple technique for independently characterizing the thickness and (anisotropic) dielectric constant(s) of optically transparent thin films.[21] To take advantage of the surface sensitive character of this method, some authors have tried to use the SPR technique to monitor self-assembly[32,33] of preformed PBLG in solution and molecular ordering[16] of end-grafted PBLG chains deposited in the vapor phase. In this work, the changing optical response of growing PBLG chains was monitored similarly by SPR and then analyzed by Fresnel calculations, to determine polypeptide layer thicknesses and dielectric responses. Furthermore, the SPR data were complemented by ex situ measurements of the polypeptide's secondary structure with Fourier transform infrared spectroscopy (FT-IR), and the final film morphology was determined with atomic force microscopy (AFM).

Experimental Section

Materials and Characterization. The *N*-carboxy anhydride of the benzyl-L-glutamate (BLG-NCA) monomer of PBLG was synthesized by phosgenation of L-glutamic acid (Merck Biosciences) with stoichiometric quantities of triphosgene (Sigma-Aldrich) in dry ethyl acetate (Fluka). Then, the monomer was purified twice by recrystallization in *n*-hexane. ^{1}H NMR spectra were recorded on a Bruker Dpx250 spectrometer, using the residual proton resonance signal of deuterated dichloromethane (CD_2Cl_2) as the internal standard: ^{1}H NMR (CD_2Cl_2, 250 MHz) δ 2.17 (m, β-CH_2), 2.52 (m, γ-CH_2), 4.32 (t, C-H), 5.14 (s, CH_2-benzylic), 6.31 (s, N-H), 7.41 (s, Ar−H). (**Caution**: *Triphosgene decomposes to highly toxic phosgene on heating and upon reaction with any nucleophile. Even a trace of moisture leads to the formation of phosgene.*[22] *Therefore, work with this substance should be conducted in a highly ventilated fume hood to prevent exposure, and the reaction byproduct should be neutralized immediately.*)

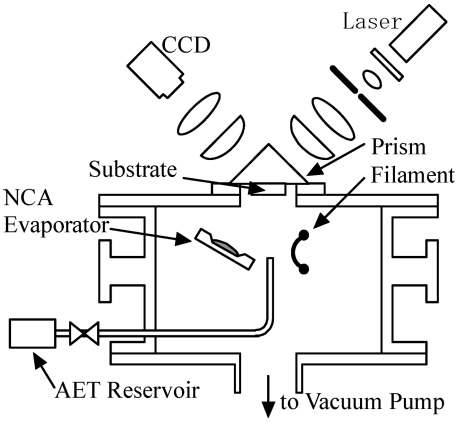

Figure 1. Schematics of the deposition setup coupled with SPR spectroscopy.

2-Aminoethanethiol (AET) (Sigma-Aldrich) was used as the initiator. AET was used without purification as obtained from the supplier. Dichloroacetic acid (≥99%, Acros Organics), chloroform (Merck), and anhydrous tetrahydrofuran (THF) (Acros Organics) were used as received.

Substrates. Glass substrates (BK7) were cut into 25 mm × 25 mm pieces and sonicated in a 2% Hellmanex solution (Hellma Optik). Cr (2 nm) followed by 50 nm Au was deposited as an optical coupling layer by thermal evaporation, each at a rate of 0.1 nm/s under a vacuum of $\sim 1 \times 10^{-4}$ Pa. The gold-coated substrate was used for AET modification.

Self-Assembled Monolayer (SAM) for Formation of the Initiator Layer. A 1 mM 2-aminoethanol (AET) solution in anhydrous ethanol was stirred for 20 min and filtered through a 0.2 μm polytetrafluoroethylene (PTFE) syringe filter before being used. Then, the bare gold substrates were immersed in an AET solution for 15 h. Afterward, the substrates were washed with ethanol and sonicated in acetone for 30 min to remove physisorbed initiator molecules.

Physical Vapor Deposition (PVD) of the Initiator. The AET initiator was also deposited by a hot filament-assisted PVD system[20] schematically shown in Figure 1. The vacuum chamber was evacuated down to 2×10^{-3} Pa, in which the AET vapor was introduced with a stainless steel tube with an outer diameter of 3 mm through a needle valve. The end of the tube was located 5 cm from the gold-coated substrate, which was attached to the bottom of a prism with index-matching oil. A tungsten hot filament, 0.2 mm in diameter and 4 cm in length, was placed near the exit of the stainless steel tube and was heated with a current of 3.5 A at 4 V.

Physical Vapor Deposition (PVD) of the BLG-NCA Monomer. The same vacuum system as described above was used for the PVD of BLG-NGA on the substrates functionalized with the initiators. The BLG-NCA monomer (5−10 mg) was charged in an evaporator boat, and freshly prepared initiator-functionalized substrates was placed on top of the monomer source at a distance of 5 cm. After the system parameters had been adjusted and the entire setup checked, the chamber was evacuated down to 2×10^{-3} Pa and the evaporator boat was heated to 100−110 °C. The vacuum pressure during the evaporation was $3-4 \times 10^{-3}$ Pa. The substrate temperature was kept at 10 °C by circulating chilled water around the substrate holder.

(14) Chang, Y.-C.; Frank, C. W. *Langmuir* **1998**, *14*, 326–334.
(15) Lee, N. H.; Frank, C. W. *Langmuir* **2003**, *19*, 1295–1303.
(16) Chang, Y.-C.; Frank, C. W.; Forstmann, G. G.; Johannsmann, D. *J. Chem. Phys.* **1999**, *111*, 6136–6143.
(17) Wu, J.-C.; Wang, Y.; Chen, C.-C.; Chang, Y.-C. *Chem. Mater.* **2008**, *20*, 6148–6156.
(18) Wang, W.; Chang, Y.-C. *J. Am. Chem. Soc.* **2003**, *125*, 6376–6377.
(19) Fulghum, T. M.; Yamagami, H.; Tanaka, K.; Usui, H.; Shigehara, K.; Advincula, R. C. *Polym. Mater.: Sci. Eng.* **2002**, *86*, 196–197.
(20) Tamada, M.; Omichi, H.; Okui, N. *Thin Solid Films* **1994**, *251*, 36–39.
(21) Knoll, W. *Annu. Rev. Phys. Chem.* **1998**, *49*, 569–638.
(22) Damle, S. B. *Chem. Eng. News* **1993**, *71*, 4.

A cleaning post-treatment was also investigated: test substrates were incubated in a 2/8 (v/v) dichloroacetic acid (DCA)/chloroform solution (pH 5.0) for 18 h, washed with copious amounts of chloroform and THF and dried with Ar.

Grafting of Poly(γ-benzyl-L-glutamate) to the Solid Substrates by BLG-NCA Polymerization via PVD. Three different strategies were followed for the growth of polypeptide films: (I) SAM of the initiator layer and PVD of the BLG-NCA monomer. First, solid substrates were functionalized with the liquid phase SAM technique. Then, these substrates were subjected to the standard PVD of BLG-NCA as stated above. (II) PVD of the initiator molecule and followed by PVD of the BLG-NCA monomer. First, the initiating layer of AET was deposited by hot filament-assisted PVD, and then BLG-NCA monomers were deposited successively by standard PVD as described above. (III) Co-evaporation of both the initiator and the BLG-NCA monomer by PVD. Both AET initiating molecules and BLG-NCA monomers were deposited simultaneously by combining hot filament-assisted and normal PVD.

In Situ Surface Plasmon Resonance Spectroscopy (in situ SPR). A customized instrument setup in the Kretschmann configuration[21,23−25] was employed to monitor the growth of the thin films deposited on the Au layer. In the Kretschmann configuration, the back side of the glass substrate is attached to the base of a symmetric glass prism (with a dielectric constant identical to that of the glass substrate) with optical immersion oil. A HeNe laser (λ = 632.8 nm) was then irradiated through the prism substrate to impinge on the thin Au metal coupling layer between the polypeptide thin film and the substrate and reflected. At a specific angle, θ, determined by the thickness and the dielectric constants of the polypeptide film, the laser was coupled with the surface plasmon resonance at the Au−PBLG interface, giving a sharp minimum in the reflected intensity (R) versus θ curve. In this work, the reflectance was monitored online by using a charge-coupled device (CCD) camera instead of via mechanical scanning of the incidence angle. The laser beam passed through a polarizer and a beam expander and then was focused onto the substrate by using a cylindrical lens. The reflected beam was shaped by another cylindrical lens and focused onto the CCD surface so that the spatial position on the CCD plane corresponds to the incident angle, θ. This method can span only a limited range of angles and also lacks angular accuracy but enables observation of the SPR spectra at a video rate. The SPR spectra are then used to determine the optical thickness of the initiator and PBLG layers by a simulation based on Fresnel calculation. From the angular shift of the SPR reflectivity minima, the film thickness was derived by Fresnel calculations, which exactly describe the layered geometry of the thin film in the Kretschmann configuration.[22,25]Tracking the coupling angle of the SPR curve enabled real-time, in situ monitoring of changes in the thickness or the dielectric constant of the film.[22] For a precise quantitative analysis and better curve fitting, the nonlinearity of the CCD camera response was taken into account by multiplication of all experimental data points, $\mathrm{Au}(\theta)^{\mathrm{CCD}}$, with a correction function, $f(\theta)$. For instance, regular reflectivity measurement was performed on substrates with similar Cr and Au layer thicknesses by a photodiode, $\mathrm{Au}(\theta)^{\mathrm{PD}}$. Where $f(\theta)$ is

$$f(\theta) = \frac{\mathrm{Au}(\theta)^{\mathrm{PD}}}{\mathrm{Au}(\theta)^{\mathrm{CCD}}} \quad (1)$$

Then, data fit curves were multiplied with the correction function, $f(\theta)$.

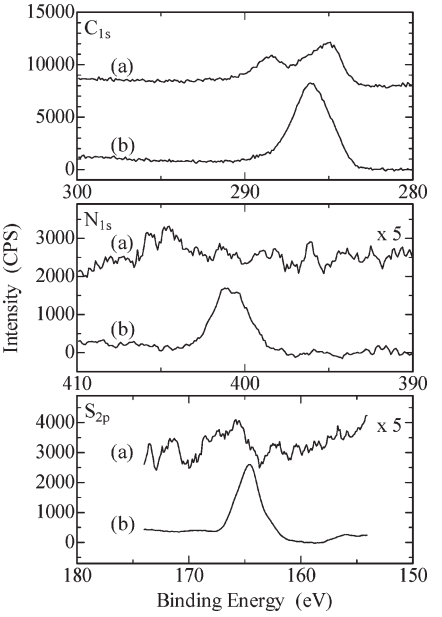

Figure 2. XPS spectra of C(1s), N(1s), and S(2p) of (a) SAM and (b) PVD-AET on a Au substrate.

Atomic Force Microscopy (AFM) Analysis. The surface morphology of the deposited films was examined by using a KEYENCE VN-8000 scanning microscope in the damping force mode.

Fourier Transform Infrared Spectroscopy (FT-IR). FT-IR spectra were recorded in reflectance mode on a Horiba FT-730 spectrometer for secondary structure investigation. For each sample, 400 scans were taken at a resolution of 2 cm^{-1} by the reflection−absorption mode (incident angle of 80°) on Au-coated substrates. The backbone amide I and amide II bands of the three most frequently occurring conformations of PBLG, i.e., α-helix (amide I at ∼1650 cm^{-1} and amide II at ∼1546−1550 cm^{-1}), β-sheet (amide I at ∼1625 or 1630 cm^{-1} and amide II at ∼1530 cm^{-1}), and random coil (amide I at ∼1658 or 1670 cm^{-1} and amide II at ∼1535 cm^{-1}), appear at distinct positions in the IR spectrum.[1,3,14,26] The characteristic peptide peaks were calculated by deconvolution of the amide I and amide II regions using Gauss−Lorentzian fitting.

X-ray Photoelectron Spectroscopy (XPS). The substrates modified either with an initiator of SAM or by PVD were characterized by XPS analysis (Shimadzu ESCA-850) after the surface had been lightly etched with an argon ion beam. The measurement was taken for C(1s), N(1s), and S(2p) electrons to confirm the existence of the initiator molecules qualitatively.

Results and Discussion

SAM of the Initiator Layer and PVD of the BLG-NCA Monomer. To obtain a monolayer with amino end groups, clean substrates were dipped in a dilute solution of the initiator molecule (AET) in anhydrous ethanol. This molecule was chosen to attach the BLG-NCA monomer to the solid substrate with one end, while keeping the NH_2 chain end active for further polymerization. A uniform film of the initiator layer was formed as confirmed by an XPS study as shown in Figure 2, curve a. The XPS signals from the monolayer were weak and relatively noisy. However, it is clear from the rough positions of the binding peaks, corresponding to the C(1s), N(1s), and S(2p) positions, that AET had been deposited. XPS gave the qualitative evidence of the

(23) Kretschemann, E. *Opt. Commun.* **1972**, *6*, 185–187.
(24) Raether, H., Kretschemann, E., Eds. *Surface Plasmons on Smooth and Rough Surfaces and on Gratings*; Springer Tracts in Modern Physics Series; Springer-Verlag: Berlin, 1988; Vol. *11*.
(25) Raether, H. *Surface Plasmons on Smooth and Rough Surfaces and on Gratings*; Springer-Verlag: Berlin, 1988; Vol. *11*.
(26) Wieringa, R. H.; Siesling, E. A.; Werkman, P. J.; Angerman, H. J.; Vorenkamp, E. J.; Schouten, A. J. *Langmuir* **2001**, *17*, 6485–6490.

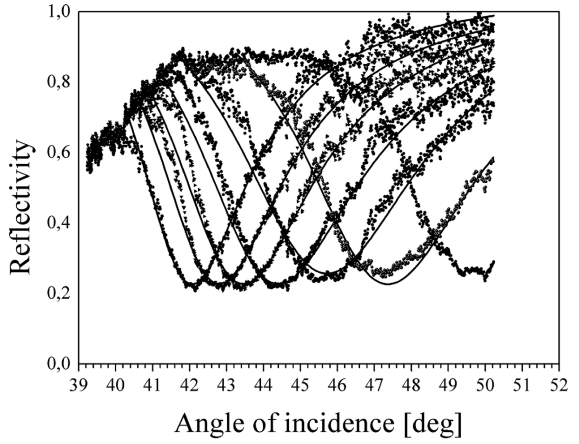

Figure 3. SPR spectroscopy of PBLG films grown with SAM-EAT on a gold substrate as a function of time. Spectra were measured every 2 min. The solid line is the fit of Fresnel calculation where the complex dielectric constant (ε) for a 45 nm Au film is $-13.6175 + 1.685i$, for an AET film 2.1025, and for a PBLG layer 2.4335.

presence of C(1s) with a binding energy of 285 eV, N(1s) with a binding energy of 404 eV, and S(2p) with a binding energy of 165 eV. Surface grafting by surface-initiated, ring opening polymerization of BLG-NCA monomers on AET-functionalized gold substrates was characterized in situ by SPR. Figure 3 shows the shifts in the SPR curve for PBLG growth on the AET-SAM layer during BLG-NCA monomer PVD. The SPR reflectivity curve at time zero exhibited a broad minimum at 42.15° at which there is only SAM AET layer on the gold surface. Fresnel calculation fits are plotted in the figure as solid lines. The AET layer thickness was measured as 0.93 nm by assuming a refractive index n_{AET} of 1.45 which indicates formation of a complete monolayer since the molecular length of AET is 0.57 nm.[27] The attachment of the BLG-NCA monomer to AET-SAM resulted in a shift in the SPR angle of 0.748° at the end of the 2 min polymerization time. This angular shift (θ) of 0.748° was converted to a PBLG layer thickness of 3.5 nm ($n_{PBLG} = 1.55$). The following spectra were measured every 2 min. The resonance angle shift can clearly be observed, indicating the stable growth of the PBLG thin film. In situ SPR measurement yielded an angle shift upon PBLG film formation of 7.84° after the 15 min monomer deposition time which gives a total PBLG film thickness of 26.2 nm. The PBLG film obtained with this approach produced a very rough film morphology. AFM observation showed that the arithmetic mean surface roughness (R_a) of the film was ~8 nm.

FT-IR spectra of the neat BLG-NCA monomer, BLG-NCA films deposited on bare Au, and BLG-NCA films deposited on a SAM-AET layer are shown in Figure 4. Anhydride carbonyl and the benzyl ester peaks in the FTIR spectrum appeared at 1860 and 1800 cm^{-1} and at 1732 cm^{-1} for the bulk BLG-NCA monomer[4] and the film deposited on the bare Au surface (panels a and b of Figure 4, respectively). On the other hand, when BLG-NCA was deposited on the AET-modified surface (Figure 4c), anhydride carbonyl peaks disappeared while new peaks at 1650 and 1550 cm^{-1} were formed corresponding to amide I (backbone carbonyl stretch) and amide II (C−N stretch and N−H deformation), respectively. The benzyl ester from PBLG side groups at 1732 cm^{-1} overlaps with the benzyl ester peak of BLG-NCA.

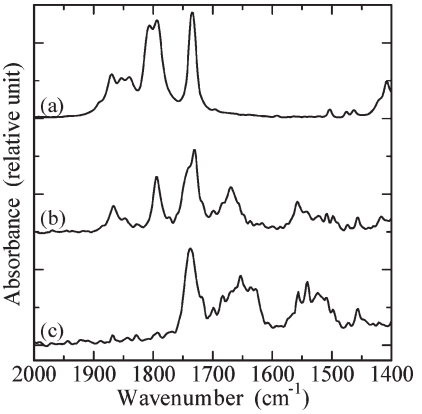

Figure 4. IR spectra of (a) neat BLG-NCA monomer, (b) PVD films of BLG-NCA deposited on bare Au, and (c) PVD films of BLG-NCA deposited on a SAM-AET layer.

The characteristic amide I and amide II peaks correspond to the α-helix conformation. Since no characteristic peaks of BLG-NCA anhydride (at 1860 and 1800 cm^{-1}) are present in the spectrum as shown in Figure 4c, this result indicates that all BLG-NCA monomers effectively polymerized on the amine-functionalized surface. The absorbances and positions of the amide I and amide II peaks corresponding to the different conformers were obtained by deconvolution of the spectra around the amide I and amide II regions using Gauss−Lorentzian fitting. Note that contributions corresponding to the aromatic ring (assumed to be centered at 1498 and 1516 cm^{-1})[28] were discounted when absorbances were calculated from the amide II regions in the deconvolution procedure. Furthermore, the spectra shown in Figure 4 were normalized according to the peak intensity of the side chain carbonyl stretch at 1730−1738 cm^{-1}, which is considered to be invariant with respect to secondary structure.[3] Thus, Figure 4 shows only the relative contributions of the secondary structures (i.e., α-helix and β-sheet) and not their absolute amounts.

PVD of the Initiator Followed by PVD of the BLG-NCA Monomer. Compared to the SAM method, a multilayered AET functional layer was formed by hot filament-assisted deposition with a film growth rate of 0.017 nm/s at 2×10^{-3} Pa. Simple introduction of AET vapor into the vacuum chamber did not cause a deposition of the initiator film (not detectable by SPR even when the substrate temperature was reduced to 0 °C). On the other hand, uniform thin films were obtained on the gold substrate at 10 °C when the tungsten hot filament was activated by an electric current. The initiator film thickness increased with time, reaching an average film thickness of 3.2 nm as identified from SPR scan curves, keeping the refractive indices $n = 1.45$. The XPS analysis of the PVD-grown AET film is shown in curve b in Figure 2. The presence of nitrogen end atoms (402 eV), sulfur anchoring atoms (165 eV), and carbon atoms (286 eV) was confirmed. The slight difference in binding energy compared to the AET by SAM might reflect the fact that the topmost molecules of PVD films are not chemically bound to the substrate.[29] Compared to the SAM technique, the PVD-AET film has a slightly larger surface roughness ($R_a \sim 14$ nm), and the thicker layer appears to have nonbonded initiator molecules on the film surface. The advantage is that the initiator layer can be

(27) Furuki, M.; Kameoka, J.; Craighead, H. G.; Isaacson, M. S. *Sens. Actuators, B* **2001**, *79*, 63–69.
(28) Miura, Y.; Kimura, S.; Imanishi, Y.; Umemura, J. *Langmuir* **1998**, *14*, 6935–6940.
(29) Ishida, T.; Hara, M.; Kojima, I.; Tsuneda, S.; Nishida, N.; Sasabe, H.; Knoll, W. *Langmuir* **1998**, *14*, 2092–2096.

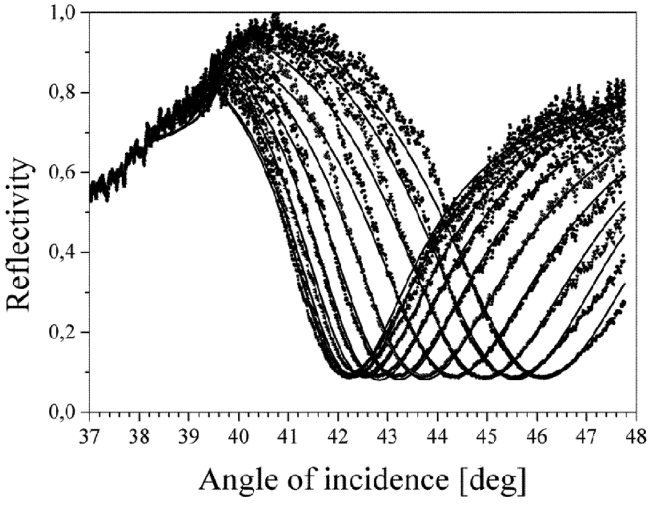

Figure 5. In situ SPR scans for PVD of BLG-NCA on AET layers deposited by hot filament-assisted PVD at a deposition pressure of 2×10^{-3} Pa. The spectra were recorded at an interval of 2 min.

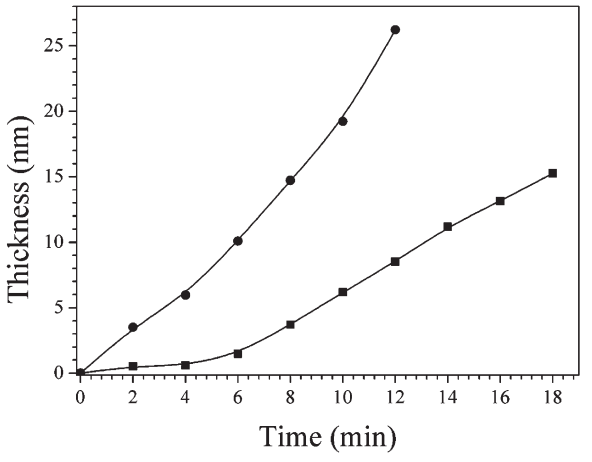

Figure 6. PBLG layer thickness change as a function of time for substrates with 0.93 nm SAM-AET (●) and 3.2 nm PVD-AET (■) initiator layers.

obtained easily in a one-batch vacuum process in the same vacuum chamber prior to BLG-NCA deposition.

To monitor the PBLG layer thickness change in real time, the shift of the angle minimum position of the SPR curve was tracked in situ, and R versus θ scans were taken every 2 min (Figure 5). There was an induction period in the first 4 min. The angle shift after surface-initiated polymerization for 4 min was 0.363°, indicating the addition of a PBLG layer with an average thickness d_{PBLG} of ~0.59 nm. Using a thickness of each BLG-NCA monomeric unit of 0.34 nm for a β-sheet[30] ($1 < DPn < 10$) conformation, it is clear that PBLG forms only a monolayer at this stage of the polymerization. The SPR minima shifted to higher angle linearly after 4 min, suggesting a regular growth of PBLG chains. The total angle shift after 18 min for surface-initiated polymerization was 4.04°, indicating the addition of a PBLG layer with an average thickness d_{PBLG} of ~15.3 nm. The corresponding increases in d_{PBLG} for PBLG films grown on both SAM-AET and PVD-AET layers, as estimated from Fresnel calculations, are shown in Figure 6.

The polymerization kinetics profiles for PBLG films grown on both SAM-AET and PVD-AET layers were compared. PBLG film thickness increased almost linearly on SAM-AET, while the thickness of PBLG films on PVD-AET showed a two-step growth profile: slower kinetics, τ_1, up to 4 min and a more profound linear increase, τ_2, after 4 min. The primary amine-initiated polymerization of BLG-NCA proceeds without the termination, because of its living polymerization characteristics. Besides, PVD polymerization of BLG-NCA is kinetically a very fast process compared to solution polymerization.[26,31−33] To understand the polymerization mechanism and follow the reaction kinetics, we needed to focus on the early stage of the deposition reaction. The final film thickness for PBLG on a PVD-AET film (15.3 nm) was smaller than that of PBLG on a SAM-AET film (26.2 nm).

Next, PBLG films were grown on thicker AET layers. The SPR shift accompanied by broadening (data not shown) suggests that the PBLG film grown on a thicker PVD-AET layer has greater optical losses. Figure 7 shows the AFM phase contrast images of the PBLG films deposited on PVD-AET layers having thicknesses of 3.2, 4.0, and 4.5 nm. The corresponding PBLG thicknesses were 15.3, 16.2, and 25.5 nm, respectively. The PBLG film on a 3.2 nm thick PVD-AET layer has a smooth surface, consistent with the regular SPR shift shown in Figure 5, whereas the films deposited on a thicker PVD-AET layer had aggregated structures giving rise to domainlike structures. The average surface roughnesses of 2.3, 2.4, and 3.0 nm were found for the increasing thicknesses of PBLG films. The PBLG film grown on a PVD-AET layer with a 4.0 nm film thickness had domains ($R_a = 25$ nm) with regular striation-like morphology. On the other hand, the PBLG film grown on a 4.5 nm AET initiator layer had larger domains ($R_a = 41$ nm) forming hexagonal arrays. It is clear that a thinner AET layer favors more uniform and higher film quality. The rough surface of these PVD films might be caused by aggregation after film deposition. If the AET layers are not bound strongly to the substrate surface, the polypeptide grown on the loose AET undergoes aggregation slowly after the deposition.

Co-Evaporation of both the Initiator and the BLG-NCA Monomer by PVD. The results described in the previous section suggest that the AET molecules that are not bound to the Au surface are more dominant in the thicker PVD-AET layer. They function in a different manner by enhancing the polymerization of NCA. It is significant in this respect to demonstrate PBLG films by co-evaporation of the BLG-NCA monomer with the AET initiator. The polymerization proceeds with uniformly dispersed initiator molecules instead of surface-tethered cites. Simultaneous deposition of the dry initiator and BLG-NCA monomer by the hot filament-assisted method was used as an alternative technique to compare film quality (roughness, order, and crystallinity). Thus, BLG-NCA was deposited at various loading pressures (3.5, 8.8, and 9.7×10^{-3} Pa) of AET to determine the effect of initiators dispersed in the film.

The film growth process during the codeposition of BLG-NCA and AET was monitored by in situ SPR as shown in Figure 8. Within a few minutes of the beginning of the deposition of BLG-NCA, the SPR peak shifted to a higher angle with the elapsing of deposition time. The curves were fitted quite well with the refractive indices of $n = 1.511$ for PBLG. Compared to the growth on predeposited AET, the film growth by codeposition at 8.8 and 9.7×10^{-3} Pa appeared to have an induction time before the onset of constant film growth due to the lack of

(30) Brown, L.; Trotter, I. F. *Trans. Faraday Soc.* **1956**, *52*, 537.

(31) Lau, H. K. A.; Duran, H.; Knoll, W. *J. Phys. Chem. B* **2009**, *113*, 3179–3189.
(32) Williams, A. J.; Gupta, V. K. *J. Phys. Chem. B* **2001**, *105*, 5223–5230.
(33) Williams, A. J.; Gupta, V. K. *Thin Solid Films* **2003**, 228–234.

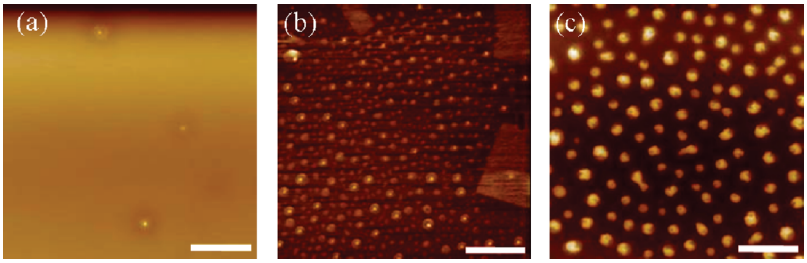

Figure 7. Phase contrast images of the PBLG films on gold substrates with an AET initiator layer by (a) SAM and by PVD with layer thicknesses of (b) 4.0 and (c) 4.5 nm. The scale bar is 10 μm.

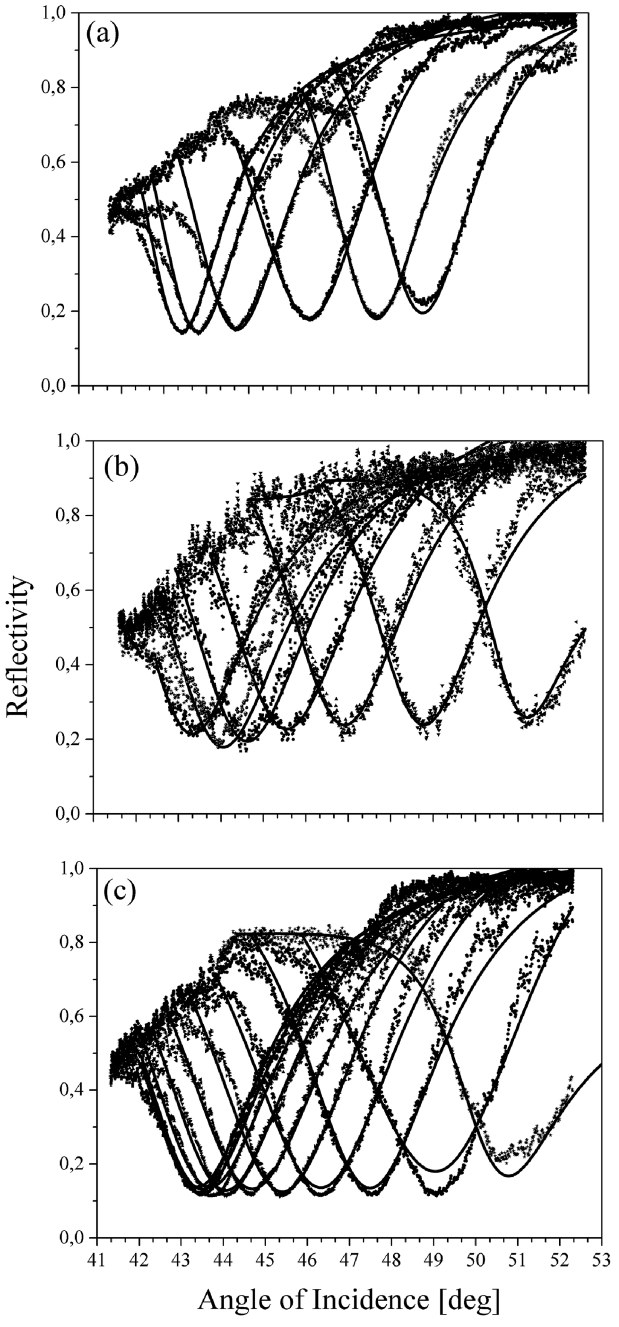

Figure 8. In situ SPR scans for co-evaporation of AET/BLG-NCA via hot filament-assisted PDV on gold surfaces. BLG-NCA was evaporated at 100 °C under the AET supply pressure of (a) 3.5×10^{-3}, (b) 8.8×10^{-3}, or (c) 9.7×10^{-3} Pa.

initiators on the substrate surface (Figure 8b,c). After 2 min, the magnitude of the angle shift becomes larger while peaks become slightly broader. Unlike surface-grown PVD-AET films, the AET film thickness remained constant during the course of deposition. The average AET layer thickness was 1.27 ± 0.15 nm for all pressures. The broadening of the peak width was not as prominent as in the case of deposition on the thick PVD-AET layer. The final surface morphologies of the corresponding films were also investigated using AFM (Figure 9). The domain size is smaller for higher deposition pressures. Besides this, the density of domains is also higher for higher pressures. It appears that the final film morphology and chain density were controlled by the amount of initiator deposited, which can be adjusted by the initiator loading conditions (i.e., pressure and temperature). This control can lead to the formation of large domains at low pressures with small and dense domains at higher pressures. Another important advantage was that the co-evaporated film had a much smoother surface (R_a = 18.9 nm) compared with the BLG-NCA film deposited on predeposited AET.

The effect of AET loading pressure on the PBLG film thickness as a function of time is displayed in Figure 10. An exponential growth profile was observed for all pressure conditions. The polymerization rate for AET deposition pressure at 3.5×10^{-3} Pa was much faster than others, giving a thicker PBLF film at the shortened times. PBLG films deposited, on the other hand, at 8.8 and 9.7×10^{-3} Pa had an almost parallel growth profile. The final film thicknesses were very close to each other, 28.1 and 25.6 nm, respectively at the end of the polymerization. In similar high-vacuum deposition studies, the PBLG film thickness was found to be slightly higher than our values.[13,15−18] For instance, in Chang's study,[17] the thickest PBLG film was 52.7 nm for the film deposited at 10^{-3}−10^{-4} Pa and at a reaction temperature of 102 °C for a deposition time of 60 min. In our work, similar pressure and temperature ranges were used, but the distance from the monomer source to the initiator-coated substrate (50 mm) was much longer than in the previous systems (4−15 mm).[13,15−17] Since we aimed to focus on the investigation of reaction kinetics at the early stage of polymerization, relatively shorter deposition times (18−20 min) were used compared to those in previous studies (30−120 min).[15−17] In addition, extremely low substrate temperatures (10 °C) were used compared with those in previously reported studies (25−60 °C).[13,18] Since all these parameters (pressure, temperature, deposition time, monomer−substrate distance, and substrate temperatures) control the final film thickness, it is hard to compare our finding with the previous results. One should also keep in mind that different substrates (gold) and initiator systems were used compared with those in previous studies [Si_2O and aminopropyltriethoxy silane (APS)], which may also have a strong influence on the PBLG growth kinetics.

The anticipated chemical shifts and changes in secondary structure during PBLG film formation were identified by FT-IR. Figure 11 shows the IR scans for the BLG-NCA monomer and the PBLG films codeposited with AET under different

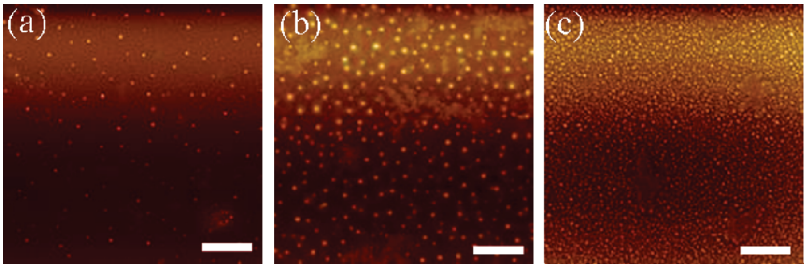

Figure 9. Phase contrast images of the PBLG films on gold substrates by codeposition of BLG-NCA with AET at AET partial pressures of (a) 3.5×10^{-3}, (b) 8.8×10^{-3}, and (c) 9.7×10^{-3} Pa. The scale bar is 10 μm.

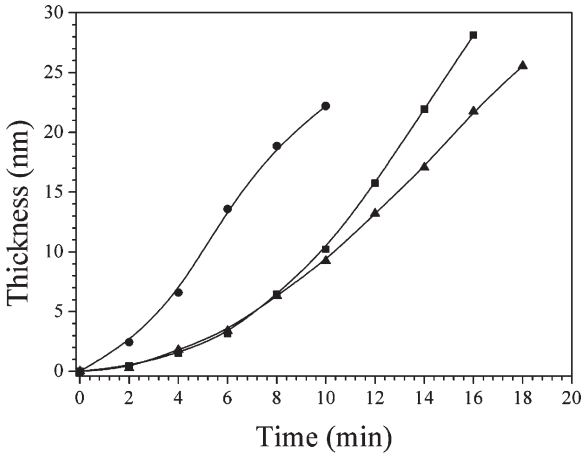

Figure 10. PBLG layer thickness change as a function of time for PVD co-evaporation of AET and NCA-BLG at 3.5×10^{-3} (●), 8.8×10^{-3} (■), and 9.7×10^{-3} Pa (▲).

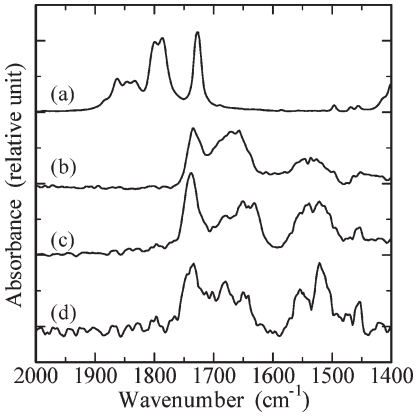

Figure 11. FT-IR spectra of (a) the BLG-NCA monomer and AET/BLG-NCA codeposited films on gold substrates at AET loading pressures of (b) 3.5×10^{-3}, (c) 8.8×10^{-3}, and (d) 9.7×10^{-3} Pa.

loading pressures. In the IR spectra, the BLG-NCA monomer has anhydride peaks from the neat monomer at 1740, 1800, and 1855 cm^{-1}. For an AET loading pressure of 3.5×10^{-3} Pa, in the amide I region (1600−1700 cm^{-1}), there is one strong and broad peak at 1650 cm^{-1}, which shows that α-helical chains had already formed on the surface. The amide II region (1500−1600 cm^{-1}), on the other hand, was relatively weak, but as the AET partial pressure increased, the characteristic amide II peaks became more visible. This resulted in double maxima for the amide II region at ~1525 and 1550 cm^{-1}, corresponding to mixtures of α-helix and β-sheet conformations.

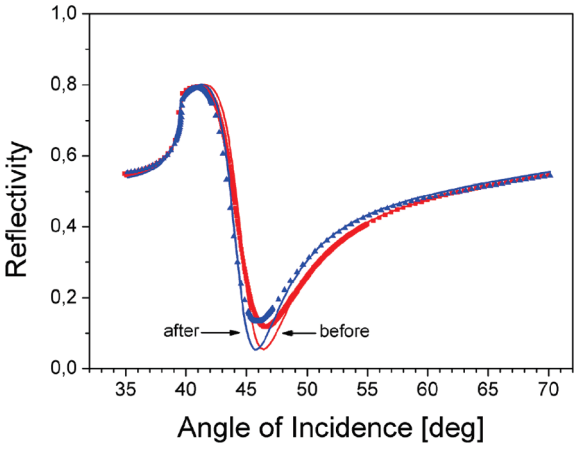

Figure 12. Shift in the SPR angle before and after a postcleaning treatment for PVD of BLG-NCA on an AET layer deposited on gold substrates at 7.4×10^{-3} Pa and 100 °C. The symbols are the experimental data, and solid lines are fits using Fresnel calculations.

To remove any physisorbed material that might have remained after the PBLG-grafted AAO template had been washed with anhydrous THF and to investigate the contribution of the physisorbed material to the overall PBLG layer, we performed an ex situ cleaning post-treatment.[18,19] The post-treatment consisted of keeping the PBLG film on PVD-AET in a DCA/chloroform mixture (20/80, v/v) for 18 h (see Experimental Section). After samples has been washed with THF and dried under Ar, the reflectivity curves of a 15.77 nm thick PBLG film on gold substrate deposited at 7.4×10^{-3} Pa and 100 °C for 20 min were obtained (Figure 12). The spectra before and after post-cleaning were recorded with ex situ SPR experiments as well as the Fresnel curve fits. The 15.77 nm thick PBLG film before cleaning had a resonance minimum of ~46.7°. After the post-treatment, on the other hand, the resonance minimum shifted toward a smaller angle of 45.8° ($\Delta\theta = -0.8°$), corresponding to a PBLG film thickness of 11.8 nm. It seems that ~25% of the PBLG chains which are not covalently attached to the substrate were removed from the surface after the post-treatment. The amount of physisorbed chains varies with deposition technique; it is 11−15% for SAM-AET and PVD of BLG-NCA, while this value becomes larger (25−35%) for films that deposited with PVD-AET and PVD of BLG-NCA.

Orientation of PBLG Chains on Gold Substrates. In addition to the conformation analysis, IR spectroscopy can be used to study the orientation and chain density of α-helical polypeptides.[14,26,28,34] In an α-helix structure, the amide I transition moment is oriented roughly parallel to the backbone axis

(34) Wang, Y.; Chang, Y. C. *Adv. Mater.* **2003**, *15*, 290–293.

because of intramolecular hydrogen bonding, while the amide II transition moment is roughly perpendicular to the backbone axis. In contrast, the orientations are reversed in a β-sheet structure; i.e., the amide I band is perpendicular to the backbone axis, while the amide II band is parallel. Thus, the PBLG orientation in the film, for either the α-helix or the β-sheet content, can be characterized by comparison of the relative absorbances of the corresponding amide I and amide II bands. (The absorbances were normalized to the side chain carbonyl stretch at 1730−1738 cm^{-1}, which is considered to be invariant to the backbone orientation.)[3] The calculation of the average tilt angle of the α-helices from the surface normal (θ) can be given by[28,35]

$$D = A_1/A_2 = K(2S_H S_1+1)/(2S_H S_2+1) \quad (2)$$

$$S_H = \frac{1}{2}(3\cos^2\theta - 1) \quad \text{and} \quad S_i = \frac{1}{2}(3\cos^2\gamma_i - 1) \quad (3)$$

where D is the dichroic ratio, A is the observed absorbance calculated from integrating each amide peak after elimination of the aromatic ring centered at 1498 cm^{-1} and at 1516 cm^{-1}, and S_H and S_i are the orientational order parameters of the helical axis and the transition moments, respectively. The subscripts refer to the amide I and amide II peaks of the α-helix conformation. K is a proportionality constant that relates the intrinsic oscillator strengths of the amide I and amide II vibrational modes. Its reported value of 1.5 ± 0.2 has been calculated from the amide I: amide II absorbance ratio as measured for a KBr pellet prepared with randomly oriented α-helical PBLG.[26,36,37] Lastly, γ_i values represent the angles between the helical axis and the transition moments of the amide I and amide II vibrations: $\gamma_I = 39°$ and $\gamma_{II} = 75°$.[22,32]

For BLG-NCA polymerization on a SAM-AET surface, the average α-helix tilt angle was found to be 36° with respect to the gold surface. On the thicker AET surfaces prepared via the PVD technique using the identical polymerization conditions, the tilt angle increased significantly to 51.2 ± 2° with respect to the surface, which is slightly higher than reported values.[11,14,26,35] For example, Wieringa[26] obtained a value of 32 ± 5° with respect to the substrate, while Chang and Frank[14] reported values of $<45°$ for vapor phase-deposited PBLG films. Moreover, Enriquez and Samulski[35] calculated a theoretical orientation of 37° for perfectly ordered helices arrayed on a surface. On the other hand, the peptide chain tilt angle from the surface normal became smaller compared with those of thick PVD-AET surfaces. This was observed for the co-evaporation of PVD-AET and BLG-NCA at 37.8°, 41.4°, and 42.3° with deposition pressures of 3.5×10^{-3}, 8.8×10^{-3}, and 9.7×10^{-3} Pa, respectively. These differences highlight the possibility of controlled chain orientation tilt angles based on the parameters for PVD grafting.

Conclusion

In this paper, high-vacuum physical vapor deposition of the BLG-NCA monomer on gold substrates was conducted by using three different strategies. The polypeptide growth was confirmed on the PVD-AET, as well as on SAM-AET. The PBLG film on PVD-AET had rougher morphologies compared to that on SAM-AET. With PVD-AET, it was important to control the AET film thickness that is predeposited prior to PBLG growth. When the PVD-AET thickness is in the range of a few nanometers, uniform and flat growth of a smooth PBLG film was achieved. When the PVD-AET thickness exceeds 4 nm, on the other hand, the PBLG grew in large island domains. We found that the rough surface of these PVD films might be caused by aggregation after film deposition. If the AET layers are not bound strongly to the substrate surface, the polypeptide grown on the loose AET layer undergoes slow aggregation after deposition. Co-evaporation of AET and BLG-NCA, on the other hand, was much more successful in the formation of smooth polypeptide films and fine small domains. The density and size of PBLG domains were influenced by the amount of AET supply during the BLG-NCA evaporation. The molecularly dispersed initiator is thought to result in uniform polymerization of PBLG throughout the film in contrast to the case of a thick PVD-AET layer, in which the initiator molecules can diffuse into the BLG-NCA film after film deposition. In general, high-vacuum PVD is a promising method for preparing tunable polypeptide thin films via a solvent-free single-batch process. The polymerization and the film morphology can be controlled by the way the initiator is deposited or codeposited. To obtain a flat and uniform polypeptide layer bound to the substrate, we found the PVD-AET procedure with an optimized initiator thickness to be most effective.

Acknowledgment. This work was supported by the European Union, via a Marie Curie Intra-European Fellowship (MEIF-CT-2005-024731), and Japan Society for the Promotion of Science Grant-in-Aid 20360347. H.D. and S.D.B.V. gratefully acknowledge the German Research Foundation (SPP Priority Program 1369).

(35) Enriquez, E. P.; Samulski, E. T. Self-assembled α-helical polypeptide films. In *Materials Research Society Symposium Proceedings*; Materials Research Society: Warrendale, PA, 1992; Vol. *255*, pp 423−434.
(36) Niwa, M.; Morikawa, M.-a.; Higashi, N. *Angew. Chem., Int. Ed.* **2000**, *39*, 960–963.
(37) Tsubio, M. *J. Polym. Sci.* **1962**, *59*, 139–153.